



HAL
open science

Modelling of a Pressure Element for Solid Oxide Fuel Cell Stack

Boguslaw Ryczek

► **To cite this version:**

Boguslaw Ryczek. Modelling of a Pressure Element for Solid Oxide Fuel Cell Stack. Fuel Cells, 2010, 10 (4), pp.676. 10.1002/fuce.200900209 . hal-00552372

HAL Id: hal-00552372

<https://hal.science/hal-00552372>

Submitted on 6 Jan 2011

HAL is a multi-disciplinary open access archive for the deposit and dissemination of scientific research documents, whether they are published or not. The documents may come from teaching and research institutions in France or abroad, or from public or private research centers.

L'archive ouverte pluridisciplinaire **HAL**, est destinée au dépôt et à la diffusion de documents scientifiques de niveau recherche, publiés ou non, émanant des établissements d'enseignement et de recherche français ou étrangers, des laboratoires publics ou privés.



Modelling of a Pressure Element for Solid Oxide Fuel Cell Stack

Journal:	<i>Fuel Cells</i>
Manuscript ID:	face.200900209
Wiley - Manuscript type:	Original Research Paper
Date Submitted by the Author:	18-Dec-2009
Complete List of Authors:	Ryczek, Boguslaw
Keywords:	Corrugated Pressure Element, Mathematical Simulation, Mechanical Model, Solid Oxide Fuel Cell, Structural Analysis



view

Modelling of a Pressure Element for Solid Oxide Fuel Cell Stack

B. Ryczek^{1*}

¹Institute of Power Engineering, Augustowka 36, 02-981 Warsaw, Poland

Received December 18, 2009;

[*] Corresponding author, boguslaw.ryczek@ien.com.pl

Abstract

The paper deals with the structural analysis of a corrugated pressure element for the SOFC stack. The aim of the element application is assurance of the fuel cell tightness and sufficient electrical contact between components by means of its uniform pressure. In the paper a method of the pressure element modelling is proposed and results of its behaviour analysis for different assembly condition (free ends, fixed ends and ends subjected to friction force) are presented. Vertical and horizontal stiffness of the corrugated element as a function of its geometrical parameters has been determined what facilitates computer simulation and engineering design of the element.

Keywords: Corrugated Pressure Element, Mathematical Simulation, Mechanical Model, Solid Oxide Fuel Cell, Structural Analysis

1 Introduction

Solid oxide fuel cells (SOFC) are the ones of the most promising solutions in the fuel cells technology for electrical energy production, mainly because of their high efficiency and low pollutants emission. These properties mostly depend on the working conditions including gas leak tightness and electrical contact between conductive components, i.e. cell unit and both interconnectors - cathode and anode.

An increase of the contact area between the unit cell and interconnectors is possible by suitable assembly pressure allowing reduction of the contact resistance and in consequence electrical losses in the fuel cell system [1]. However too high pressure can cause the unit cell damage, whereas uneven contact pressure distribution can be the reason of the hot spots which are detrimental for fuel cell durability [2]. In order to obtain the sufficient components pressure in the planar SOFC, screwed connections are usually applied [3--5]. As a result from the experimental investigations of the solid oxide fuel cells (conducted at the Institute of Power Engineering in Warsaw) and the theoretical analysis of the fuel cell screw joints, a clearance in the connection at the operating temperature (1073 K) has been observed. Thermal expansion of the fuel cell elements and shrinkage of gaskets make it difficult to eliminate this clearance only by increasing of the torsional moment acting on the nut.

In this paper a mechanical solution to compensate the arising clearance, ensure uniform pressure of mating elements and consequently high leak tightness as well as sufficient electrical contact in the fuel cell packet/stack, is proposed. It consists in the application of a corrugated pressure element located between top plate and cathode interconnector. In order to determine the parameters of the pressure element, the energetic method for the element modelled as a curved bar was adopted [6]. Results of the parameters designation for simpler elements - semicircle or single circular sector - have been presented in papers [7--10]. Nevertheless shapes and related parameters of these elements do not correspond to the more complex geometry of the element which will be used in the SOFC packet/stack. Therefore, detailed structural analysis was carried out and parameters of the pressure element for its various assembly cases have been determined.

2 Characteristics of Corrugated Element

2.1 Pressure element building

The proposed pressure element will be placed between the top plate which closes the fuel cell packet/stack, and cathode interconnector (see Figure 1 a). The element will be shaped as a corrugated strip, composed of successive wavy sectors, so-called corrugations (Figure 1 b). It will be subjected to the pressure originated from the screwed connection, i.e. stud bolts joining the SOFC plates. The number and

dimensions of the wavy sectors which compose the whole pressure element depend on its demanded properties, dimensions of the fuel cell and construction (single fuel cell packet or stack). Geometry of the element is described by the following basic parameters:

- width w , thickness t , height h ,
- length of the element l and of the corrugation p .

2.2 Physical Parameters of the Pressure Element and Acting Forces

The system of three SOFC components: top plate – pressure element – cathode interconnector, can be characterized by the following physical parameters:

- vertical and horizontal stiffness coefficients of the pressure element,
- friction coefficient between the pressure element and interconnector (in the case of Coulomb model),
- contact stiffness between the element and interconnector (in the case of Hertzian model).

The influence of the parameters on the interaction between the pressure element and the interconnector depend on the conditions of the element operating. In the whole range of the element working, the significant parameters are: vertical and horizontal stiffness, whereas friction on the contact surface exists to the moment of the element fully compression, while the contact deformation begins to be predominant (see Figure 2). These effects described by means of interaction forces between the mating fuel cell components, are shown in Figure 3.

3 Determination of the Pressure Element Stiffness

3.1 Wavy Sector Geometry

The pressure element considered as a set of the wavy sectors (corrugations) enables the structural analysis to be conducted. For that purpose single wavy sector has been described as a weightless curved bar consisted of circular segments which is characterized by flexural rigidity depending on material and geometrical properties (Figure 4).

The wavy sector is described by the following geometrical parameters:

$$\beta = 2\arctg\left(\frac{p}{2h}\right), \quad r = \frac{p}{4\sin(\beta)}, \quad \alpha = 2\arcsin\left(\frac{p}{4r}\right) \quad (1)$$

3.2 Wavy Sector Stiffness

Considering the sector subjected to the static load F (see Figure 4), the vertical reaction force fulfils the condition:

$$R_v = \frac{F}{2} \quad (2)$$

hence for $0 \leq \varphi_1 \leq \frac{\alpha}{2}$ bending moment takes the following form:

$$M_1 = \frac{1}{2} Fr \sin \varphi_1 - R_h r (1 - \cos \varphi_1) \quad (3)$$

and for $\frac{\pi - \alpha}{2} \leq \varphi_2 \leq \frac{\pi}{2}$:

$$M_2 = Fr \left(\sin \frac{\alpha}{2} - \frac{1}{2} \cos \varphi_2 \right) - R_h r \left(1 + \sin \varphi_2 - 2 \cos \frac{\alpha}{2} \right) \quad (4)$$

Elastic strain energy derivatives are described as follows:

$$\begin{aligned}
\frac{\partial V}{\partial R_h} &= \frac{2}{EJ} \int_0^{\frac{\alpha}{2}} \left[\frac{Fr}{2} \sin \varphi_1 - R_h r (1 - \cos \varphi_1) \right] r (\cos \varphi_1 - 1) r d\varphi_1 + \\
&+ \frac{2}{EJ} \int_{\frac{\pi-\alpha}{2}}^{\frac{\pi}{2}} \left[Fr \left(\sin \frac{\alpha}{2} - \frac{1}{2} \cos \varphi_2 \right) - R_h r \left(1 + \sin \varphi_2 - 2 \cos \frac{\alpha}{2} \right) \right] (-r) \left(1 + \sin \varphi_2 - 2 \cos \frac{\alpha}{2} \right) r d\varphi_2 = \\
&= \frac{Fr^3}{EJ} \left(\frac{1}{2} + \alpha \sin \alpha - \alpha \sin \frac{\alpha}{2} - 2 \cos \frac{\alpha}{2} + \frac{3}{2} \cos \alpha \right) + \\
&+ \frac{R_h r^3}{EJ} \left(3\alpha - \sin \alpha - 2\alpha \cos \frac{\alpha}{2} - 4 \cos \frac{\alpha}{2} \sin \alpha + 4\alpha \cos^2 \frac{\alpha}{2} \right)
\end{aligned} \quad (5)$$

and

$$\begin{aligned}
\frac{\partial V}{\partial F} &= \frac{2}{EJ} \int_0^{\frac{\alpha}{2}} \left[\frac{Fr}{2} \sin \varphi_1 - R_h r (1 - \cos \varphi_1) \right] r \left(\frac{r}{2} \sin \varphi_1 \right) r d\varphi_1 + \\
&+ \frac{2}{EJ} \int_{\frac{\pi-\alpha}{2}}^{\frac{\pi}{2}} \left[Fr \left(\sin \frac{\alpha}{2} - \frac{1}{2} \cos \varphi_2 \right) - R_h r \left(1 + \sin \varphi_2 - 2 \cos \frac{\alpha}{2} \right) \right] \left(\frac{r}{2} \right) \left(2 \sin \frac{\alpha}{2} - \cos \varphi_2 \right) r d\varphi_2 = \\
&= \frac{Fr^3}{EJ} \left(\frac{1}{4} \alpha + \frac{3}{4} \sin \alpha - 2 \sin \frac{\alpha}{2} + \alpha \sin^2 \frac{\alpha}{2} \right) + \\
&+ \frac{R_h r^3}{EJ} \left(\frac{1}{2} + \alpha \sin \alpha - \alpha \sin \frac{\alpha}{2} - 2 \cos \frac{\alpha}{2} + \frac{3}{2} \cos \alpha \right)
\end{aligned} \quad (6)$$

In the next part of the paper the deformation of the pressure element in the horizontal and vertical direction is determined. The formulae are derived for the following characteristic loading cases:

- (i) maximal horizontal reaction force (fixed element's ends),
- (ii) no horizontal reaction force (free element's ends),
- (iii) occurrence of friction force.

3.2.1 The Case of the Maximal Horizontal Reaction Force

Making use of the condition: $\frac{\partial V}{\partial R_h} = 0$, the horizontal reaction force can be written as:

$$R_h = \frac{F \left[\alpha \left(\sin \frac{\alpha}{2} - \sin \alpha \right) - \frac{1}{2} + 2 \cos \frac{\alpha}{2} - \frac{3}{2} \cos \alpha \right]}{\alpha \left(3 - 2 \cos \frac{\alpha}{2} \right) - \sin \alpha \left(1 + 4 \cos \frac{\alpha}{2} \right) + 4\alpha \cos^2 \frac{\alpha}{2}} \quad (7)$$

hence horizontal deformation of the wavy sector reads:

$$\delta_h = \frac{2\partial V}{\partial R_h} = 0 \quad (8)$$

and its vertical deformation:

$$\begin{aligned}
\delta_v = \frac{\partial V}{\partial F} &= \frac{Fr^3}{EJ} \left(\frac{\frac{7}{4} \alpha^2 - \frac{1}{4} + \sin \alpha \left(\frac{9}{4} - \alpha \right) - 5\alpha \sin \frac{\alpha}{2} + \frac{3}{4} \cos \alpha + \cos \frac{\alpha}{2} \left(2 - \frac{1}{2} \alpha^2 \right) - \sin \frac{\alpha}{2} \sin \alpha (1 - \alpha^2) - \frac{3}{2} \sin 2\alpha}{3\alpha - \sin \alpha - \cos \frac{\alpha}{2} (2\alpha + 4 \sin \alpha) + 4\alpha \cos^2 \frac{\alpha}{2}} \right) + \\
&+ \frac{Fr^3}{EJ} \left(\frac{\sin^2 \alpha \left(\frac{13}{4} - 2\alpha \sin \frac{\alpha}{2} \right) - 4 \cos^2 \frac{\alpha}{2} + \sin^2 \frac{\alpha}{2} (\alpha^2 - \alpha \sin \alpha) - 3 \sin^2 \alpha \cos \frac{\alpha}{2} + 3\alpha \sin \alpha \left(\cos \frac{\alpha}{2} + \cos^2 \frac{\alpha}{2} \right) - 3\alpha \sin^3 \frac{\alpha}{2} + 6 \cos^3 \frac{\alpha}{2}}{3\alpha - \sin \alpha - \cos \frac{\alpha}{2} (2\alpha + 4 \sin \alpha) + 4\alpha \cos^2 \frac{\alpha}{2}} \right)
\end{aligned} \quad (9)$$

3.2.2 The Case of the Horizontal Reaction Force Nonoccurrence

In the case when the horizontal reaction force $R_h = 0$, using Eqs. (5) and (6), the horizontal deflection of the wavy sector take the form:

$$\delta_h = \frac{Fr^3}{EJ} \left(1 - 3\sin^2 \frac{\alpha}{2} - 4\cos \frac{\alpha}{2} - 2\alpha \sin \frac{\alpha}{2} + 3\cos^2 \frac{\alpha}{2} + 2\alpha \sin \alpha \right) \quad (10)$$

and the deformation in the vertical direction:

$$\delta_v = \frac{Fr^3}{EJ} \left(\frac{1}{4}\alpha + \frac{3}{4}\sin \alpha - 2\sin \frac{\alpha}{2} + \alpha \sin^2 \frac{\alpha}{2} \right) \quad (11)$$

3.2.3 The Case of the Friction Force Occurrence

Assuming the Coulomb friction model to describe the contact phenomenon between the interconnector and pressing element within the range of the element working (cf. Figures 2 and 3) friction force is defined by the following equation:

$$R_h = \frac{\mu F}{2} \quad (12)$$

then taking advantage of the Eqs. (5) and (6), the horizontal and vertical deformations of the wavy sector can be written in the form:

$$\delta_h = \frac{Fr^3}{EJ} \left[\mu \left(3\alpha - \sin \alpha - 2\alpha \cos \frac{\alpha}{2} - 4\cos \frac{\alpha}{2} \sin \alpha + 4\alpha \cos^2 \frac{\alpha}{2} \right) - 3\sin^2 \frac{\alpha}{2} - 4\cos \frac{\alpha}{2} + 1 - 2\alpha \sin \frac{\alpha}{2} + 3\cos^2 \frac{\alpha}{2} + 2\alpha \sin \alpha \right] \quad (13)$$

$$\delta_v = \frac{Fr^3}{EJ} \left[\mu \left(\frac{1}{4} - \cos \frac{\alpha}{2} - \frac{3}{4}\sin^2 \frac{\alpha}{2} - \frac{\alpha}{2} \sin \frac{\alpha}{2} + \frac{\alpha}{2} \sin \alpha + \frac{3}{4}\cos^2 \frac{\alpha}{2} \right) + \frac{1}{4}\alpha + \frac{3}{4}\sin \alpha - 2\sin \frac{\alpha}{2} + \alpha \sin^2 \frac{\alpha}{2} \right] \quad (14)$$

3.3 Stiffness of the Wavy Sector and Corrugated Element

Stiffness coefficient of the wavy sector in horizontal direction is defined in the following way:

$$K_h = \frac{F}{\delta_h} \quad (15)$$

and in the vertical direction:

$$K_v = \frac{F}{\delta_v} \quad (16)$$

Considering the corrugated element model as a system composed of linear elastic elements connected in series or in parallel, and assuming constant values of stiffness coefficients of the successive corrugations in the specified directions ($K_{hi} = const = K_h$ and $K_{vi} = const = K_v$), equivalent horizontal stiffness of the pressure element reads:

$$K_{he} = \frac{1}{\sum_{i=1}^n \frac{1}{K_{hi}}} = \frac{K_h}{n} \quad (17)$$

and equivalent vertical stiffness:

$$K_{ve} = \sum_{i=1}^n K_{vi} = n K_v \quad (18)$$

4 Calculation of the Pressure Element Stiffness

4.1 Stiffness Coefficient for Different Loading Cases

Stiffness coefficients of the pressure element are the essential parameters which proper values determine correctness of the element operating in the SOFC packet/stack. The coefficients depend on the physical and geometrical parameters of the element. These parameters accepted in the stiffness calculation both for the wavy sector and whole pressure element made of high-temperature alloy, are gathered in Table 1.

In Table 2 the stiffness coefficients of the wavy sector and pressure element in the vertical and horizontal directions (K_v and K_h , respectively) are reported. They have been calculated for different loading cases at the room temperature and 1073 K allowing for the thermal expansion and change of the mechanical parameters (Young's modulus, friction coefficient). The comparison of the obtained results revealed that the stiffness of the pressure element in the vertical direction is above two times higher as the one in the horizontal direction (except the case of maximal horizontal reaction force). Moreover all stiffness coefficients at working temperature proved to be about twice lower as the ones at the room temperature.

4.2 Stiffness as a Function of Geometrical Parameters

Taking into account the existence of the friction force between the pressure element and interconnector, the stiffness coefficients of the wavy sector and the element (K_v , K_h) in relation to the geometrical parameters of the corrugation: height h and length p , have been determined. In Figures 5 and 7 the stiffness coefficients for the wavy sector and the pressure element as a function of corrugation height at its assigned length $p = 25$ mm, have been illustrated. Dependencies of these coefficients on the length of corrugation at constant value of its height $h = 8$ mm, are shown in Figures 6 and 8.

Both in the case of single wavy sector and the whole pressure element the stiffness coefficients decrease with the increase of the corrugation dimensions: h and p . At constant value of the corrugation length p and for lower height values $h < 4.3$ mm, stiffness of the wavy sector in the horizontal direction is higher as the one in the vertical direction (see Figure 5). For higher values of the corrugation height h , the vertical stiffness is higher than the horizontal one. Stiffness of the sector in horizontal direction is also lower than the vertical one in the case of fixed corrugation height for its length $p < 46.2$ mm. After this value has been exceeded, stiffness in horizontal direction is slightly higher than the vertical one.

Stiffness coefficients of the whole pressure element depend on the stiffness of its constituents, i.e. wavy sectors. The element stiffness in the vertical direction is higher than in the horizontal within the whole range of the corrugation geometrical parameters (height, length), and the difference between stiffness coefficients diminishes with the rise of these parameters values (cf. Figures 7 and 8). Increase in the corrugation length at its assigned height results in considerably higher decline of the stiffness coefficients differences than the height growth at fixed length of the wavy sector.

5 Concluding Remarks

As a result of the structural analysis of the corrugated element allowing for the energetic method in the case of the proposed model composed of curved bars in the wave-like shape, the dependency between mechanical parameters of the element (deformation, stiffness), its geometrical parameters and loading types, has been noticed. In the considered case the values of the stiffness coefficients in the vertical and horizontal direction are the smallest ones for nonoccurrence of horizontal reaction force, whereas if the force is maximal, these coefficients take the largest values. It has been also observed that in the case of the friction force action between pressure element and interconnector, these coefficients change their values with the variation of the geometrical parameters of the pressure element. For smaller values of the corrugation height its stiffness in the horizontal direction is much larger than the vertical one, while at lower values of corrugation length this relation is inverse. When increasing the geometrical parameters, after exceeding their boundary values of height and length (h_b and p_b , respectively), these relations alter. Reduction in the corrugation length at its fixed height allows substantially the increase of the stiffness in vertical direction of the whole pressure element. This result in the case of decrease of the corrugation height at its constant length is much smaller, similarly to the case of the horizontal stiffness variation at changeable corrugation length. Furthermore, comparing the outcomes obtained for the wavy sector and pressure element one can also ascertain that growth of the corrugations number causes a drop of the element stiffness in the horizontal direction and rise of its vertical stiffness. The analysis exhibited also that all stiffness coefficients at 1073 K are about two times lower as the ones at the room temperature.

One of the most significant parameter which determines the suitable operating of the pressure element in the fuel cell system (optimal pressure of the fuel cell components ensuring high leak tightness and sufficient electrical contact) is the stiffness coefficient in the vertical direction. Acceptance of its proper value during the selection of the elements physical and geometrical parameters is the condition of the correct computer simulation and design of the fuel cell packet/stack pressure system and in the consequence of the reliable SOFC performance. Therefore, further investigations into the pressure element behaviour will be devoted to the analysis of such effects influence as: assembly preload, sectors interaction, and high temperature. Experimental verification of the results obtained theoretically will be also incorporated in the study.

List of Symbols

Latin letters

E	Coefficient of elasticity for the pressure element material (Young's modulus) / GPa
F	Static force / N
h	Height of the element/corrugation / mm
J	Moment of inertia of the element cross-section / mm ⁴
K	Stiffness coefficient / MN mm ⁻¹
M	Bending moment / N mm
n	Number of the corrugations
p	Length of the corrugation / mm
r	Radius of the circular sector / mm
R	Reaction force / N
t	Thickness of the element / mm
V	Elastic strain energy / J
w	Width of the element / mm

Greek letters

α, β	Angles describing the circular sector
δ	Deflection of the wavy sector /mm
μ	Dry friction coefficient
φ	Coordinate

Sub scripts

b	Boundary value
e	Pressure element
h	Horizontal direction
i	Number of the successive corrugation
v	Vertical direction
1	First circular segment
2	Second circular segment

References

- [1] H. Yoshida, H. Yakabe, K. Ogasawara, T. Sakurai, *J. Power Sources* **2006**, *157*, 775.
- [2] S.-J. Lee, C.-D. Hsu, C.-H. Huang, *J. Power Sources* **2005**, *145*, 353.
- [3] E. N. Potter, *Fuel Cells Bulletin* **2000**, *26*, 8.
- [4] J. Duquette, A. Petric, *J. Power Sources* **2004**, *137*, 71.
- [5] M. Yokoo, Y. Tabata, Y. Yoshida, H. Orui, K. Hayashi, Y. Nozaki, K. Nozawa, H. Arai, *J. Power Sources* **2008**, *184*, 84.
- [6] G. Rakowski, R. Solecki, *Curved bars; Static calculations*, Publisher 'Arkady', Warsaw, **1965**.
- [7] C. P. Ku, and H. Heshmat, *ASME J. of Tribology* **1992**, *114*, 394.
- [8] I. Iordanoff, *Transactions of the ASME* **1999**, *121*, 816.
- [9] D. Rubio, L. San Andrés, *J. of Engineering for Gas and Power* **2006**, *128*, 653.
- [10] E. E. Swanson, *Transactions of the ASME* **2006**, *128*, 542-550.

Figure Captions

- Fig. 1 Corrugated pressure element: a) location of the element in the SOFC packet, b) basic geometrical parameters of the element.
- Fig. 2 Physical properties of the pressure element – interconnector system in different working phases.
- Fig. 3 Characteristics of the forces acting on the pressure element for the fuel cell stack.
- Fig. 4 Geometrical parameters of the wavy sector.
- Fig. 5 Stiffness of the corrugation as a function of its height at $p = 25$ mm.
- Fig. 6 Stiffness of the corrugation versus its length at $h = 8$ mm.
- Fig. 7 Dependence of the pressure element stiffness on the corrugation height at $p = 25$ mm.
- Fig. 8 Dependence between the pressure element stiffness and the corrugation length at $h = 8$ mm.

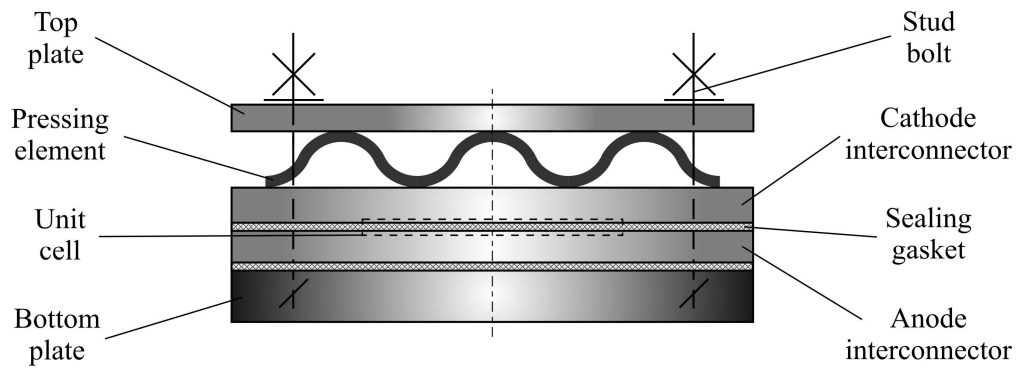
Tables

Table 1 Assumed pressure element parameters.

Parameter	Value
Width of the element / mm	20
Height of the element/corrugation / mm	8
Thickness of the element / mm	1
Length of the corrugation / mm	25
Length of the element / mm	75
Number of the corrugations	3
Arc length of the corrugation / mm	31,2
Arc length of the element / mm	93,6
Density / g cm ⁻³	8,29
Mass of the element / g	15.5
Thermal expansion coefficient at 1073 K / $\mu\text{m m}^{-1} \text{K}^{-1}$	14.9
Young's modulus at 298/1073 K / GPa	217/166
Friction coefficient at 298/1073 K	0.15/0.09

Table 2 The cases of the calculated stiffness coefficients.

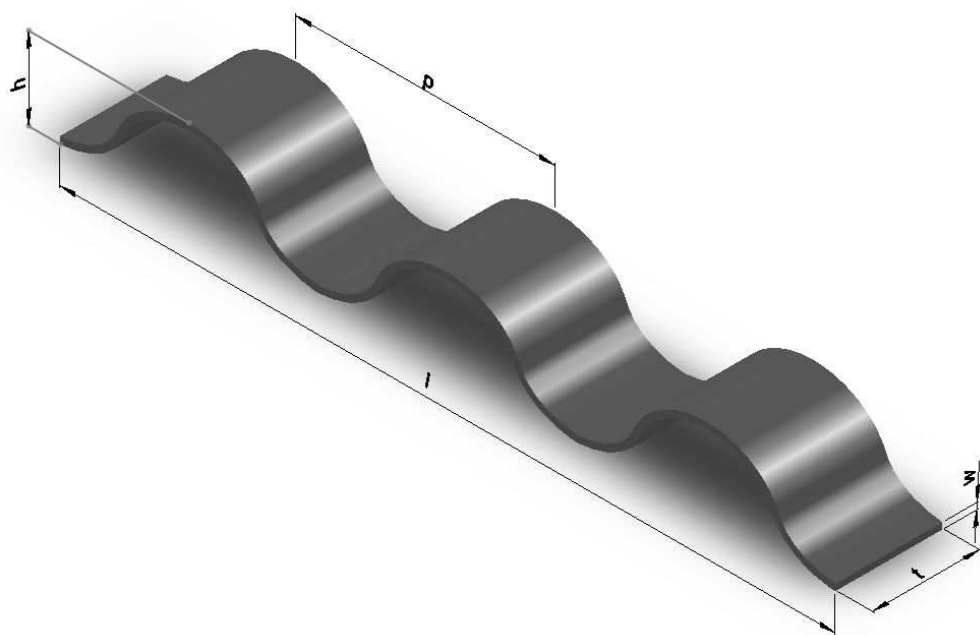
Case		Stiffness coefficient			
		vertical / MN m ⁻¹		horizontal / MN m ⁻¹	
		at 250 °C	at 800 °C	at 250 °C	at 800 °C
Wavy sector	No horizontal reaction force	0.92	0.49	0.34	0.18
	Friction force	1.03	0.52	0.42	0.20
	Maximal reaction force	3.50	1.95	∞	∞
Pressure element	No horizontal reaction force	2.77	1.48	0.11	0.06
	Friction force	3.09	1.57	0.14	0.07
	Maximal reaction force	10.49	5.86	∞	∞



Corrugated pressure element: location of the element in the SOFC packet.
244x87mm (300 x 300 DPI)

Peer Review

1
2
3
4
5
6
7
8
9
10
11
12
13
14
15
16
17
18
19
20
21
22
23
24
25
26
27
28
29
30
31
32
33
34
35
36
37
38
39
40
41
42
43
44
45
46
47
48
49
50
51
52
53
54
55
56
57
58
59
60

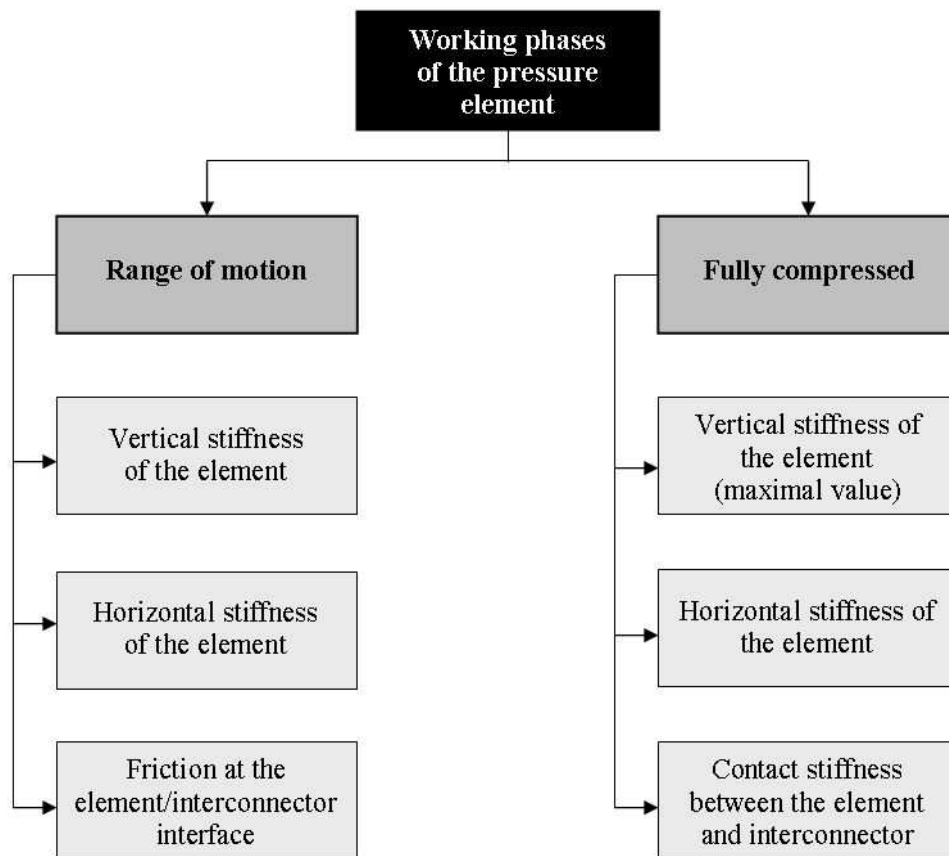


Corrugated pressure element: b) basic geometrical parameters of the element.
83x54mm (300 x 300 DPI)

Review

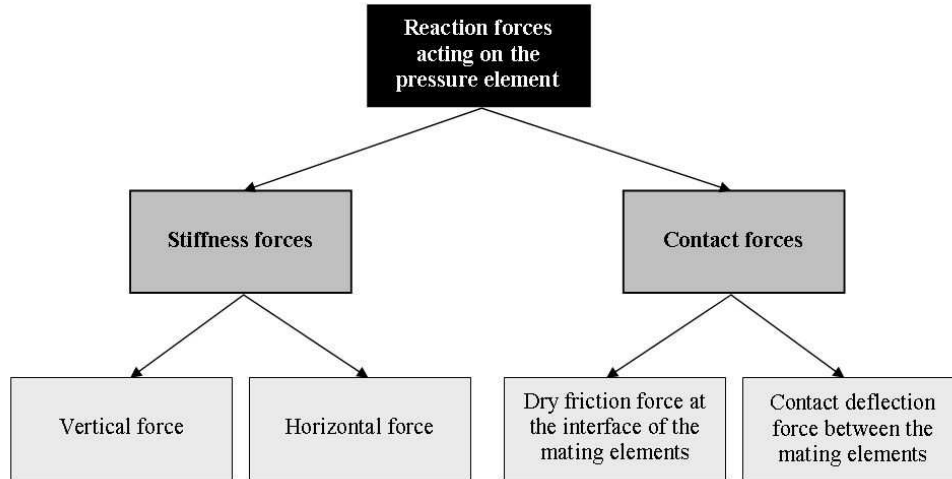
1
2
3
4
5
6
7
8
9
10
11
12
13
14
15
16
17
18
19
20
21
22
23
24
25
26
27
28
29
30
31
32
33
34
35
36
37
38
39
40
41
42
43
44
45
46
47
48
49
50
51
52
53
54
55
56
57
58
59
60

1
2
3
4
5
6
7
8
9
10
11
12
13
14
15
16
17
18
19
20
21
22
23
24
25
26
27
28
29
30
31
32
33
34
35
36
37
38
39
40
41
42
43
44
45
46
47
48
49
50
51
52
53
54
55
56
57
58
59
60



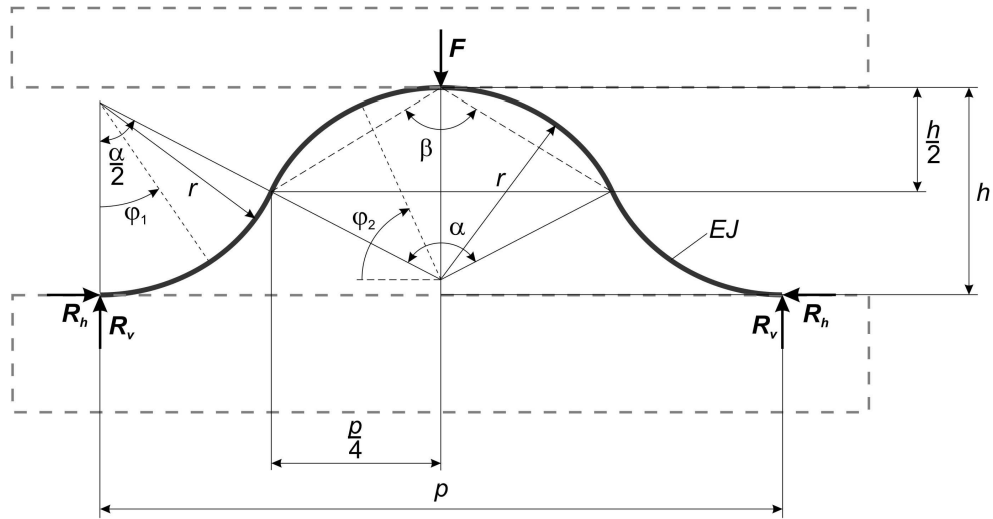
Physical properties of the pressure element – interconnector system in different working phases.
65x59mm (300 x 300 DPI)



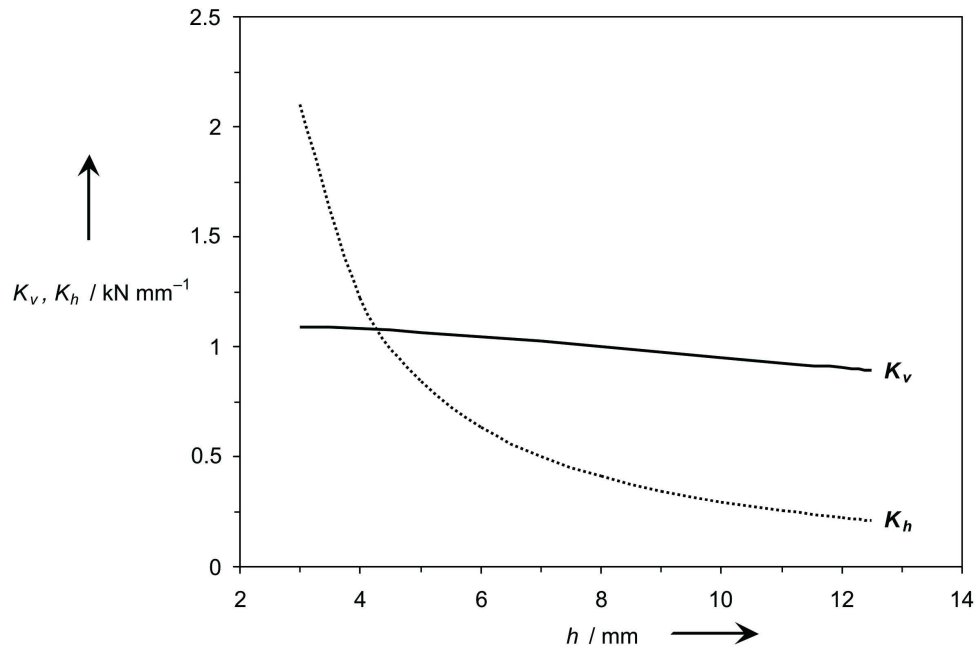


26
27
28
29
30
31
32
33
34
35
36
37
38
39
40
41
42
43
44
45
46
47
48
49
50
51
52
53
54
55
56
57
58
59
60

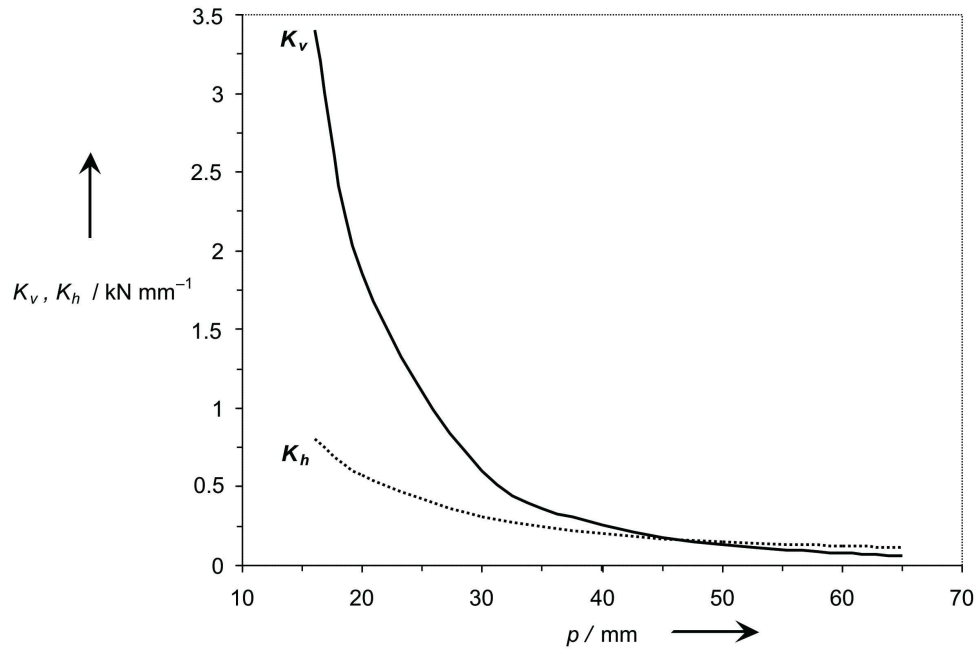
Characteristics of the forces acting on the pressure element for the fuel cell stack.
83x43mm (300 x 300 DPI)



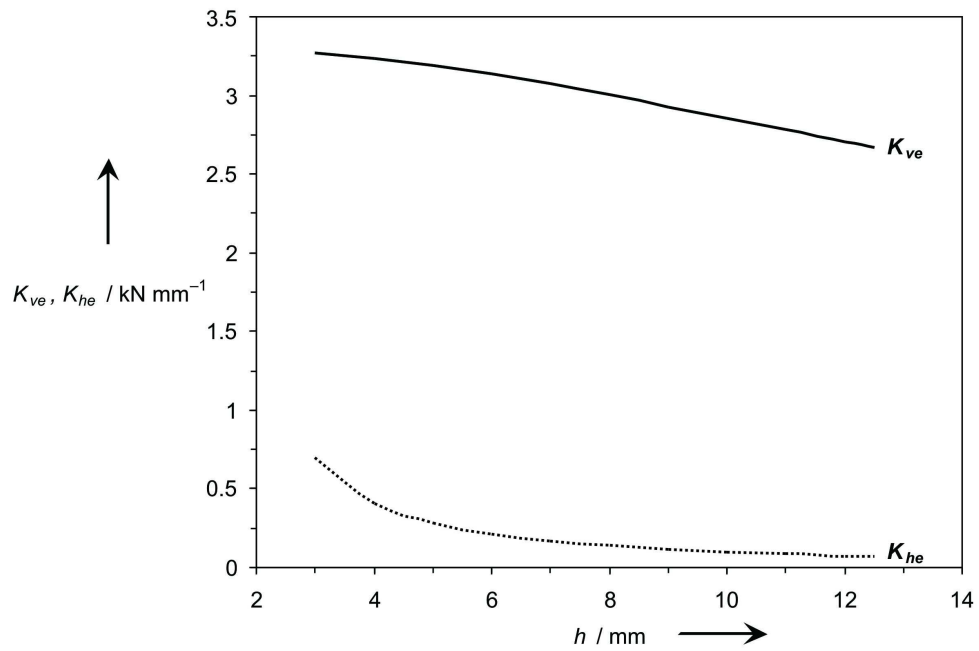
Geometrical parameters of the wavy sector.
238x128mm (300 x 300 DPI)



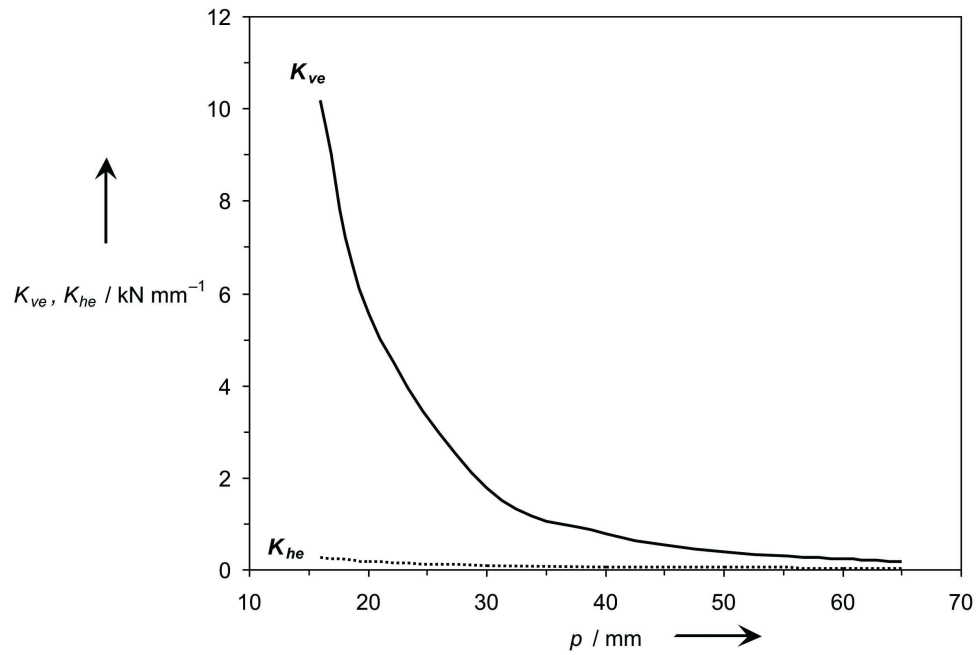
Stiffness of the corrugation as a function of its height at $p = 25$ mm.
207x142mm (300 x 300 DPI)



Stiffness of the corrugation versus its length at $h = 8$ mm.
207x142mm (300 x 300 DPI)



Dependence of the pressure element stiffness on the corrugation height at $p = 25$ mm.
207x142mm (300 x 300 DPI)



Dependence between the pressure element stiffness and the corrugation length at $h = 8$ mm.
207x142mm (300 x 300 DPI)